

Biomimetic Morphogenesis of Fluorapatite-Gelatin Composites: Fractal Growth, the Question of Intrinsic Electric Fields, Core/Shell Assemblies, Hollow Spheres and Reorganization of Denatured Collagen

Susanne Busch,^[a] Hans Dolhaine,^[b] Alexander DuChesne,^[c] Sven Heinz,^[a] Oliver Hochrein,^[a] Franco Laeri,^[d] Oliver Podebrad,^[e] Uwe Vietze,^[d] Thomas Weiland,^[e] and Rüdiger Kniep,^{*,[a][f]}

Keywords: Fractals / Materials science / Fluorapatite / Collagen / Intrinsic electric fields / Core/shell assemblies

The biomimetic growth of fluorapatite in gelatin matrices at ambient temperature (double-diffusion technique) starts with elongated hexagonal-prismatic seeds followed by self-similar branching (fractal growth) and ends up with anisotropic spherical aggregates. The chemical system fluorapatite/gelatin is closely related to in vivo conditions for bone or tooth formation and is well suited to a detailed investigation of the formation of an inorganic solid with complex morphology (morphogenesis). The fractal stage of the morphogenesis leads to the formation of closed spheres with diameters of up to 150 μm . The self-assembled hierarchical growth thereby shows immediate parallels to the topological branching criteria of the macromolecular starburst

dendrimers. A second growth stage around the closed spheres of the first stage is characterized by the formation of concentric shells consisting of elongated prismatic fluorapatite units with nearly parallel orientation (maximum diameter of the complete core/shell spheres of 1 μm). The specific structure of the core/shell assembly is similar to the dentin/enamel structure in teeth. Together with the idea of the biological significance of electric fields (pyro-, piezoelectricity) during apatite formation under in vivo or biomimetic conditions the present paper considers the composite character of the material and the mechanisms of fractal growth (branching criteria and architecture, the influence of intrinsic electric fields etc.).



Dr. Susanne Busch studied chemistry at Darmstadt University of Technology and received her Ph.D. degree under the supervision of Prof. Dr. R. Kniep in winter 1998. The thesis is entitled "Self-Organization and Morphogenesis of Apatite-Gelatin-Composites under Biomimetic Conditions." At present she is continuing her research on the topic of biomimetic growth of apatite at the Max-Planck-Institute for Chemical Physics of Solids, Dresden.

Dr. Hans Dolhaine studied chemistry at the Universities of Münster, Dortmund and Düsseldorf. He received his Ph.D. degree in 1977. The thesis entitled "NMR-studies on Phosphonates" was performed in Prof. Dr. G. Hägele's laboratories at the University of Düsseldorf, supported by a fellowship from the "Studienstiftung des Deutschen Volkes." Currently he is working on various industrial research projects at the Henkel KGaA, Düsseldorf.

Dr. Alexander DuChesne studied chemistry at the Universities of Mersburg and Sofia. In 1991 he started investigations on block copolymer morphologies at the Max-Planck-Institute for Polymer Research in Mainz under the supervision of Prof. Dr. G. Wegner. After receiving his Ph.D. degree in 1993 he went to University College, Dublin to work on conformational transitions of thermoreversible polymer gels with Prof. Dr. K. Dawson. In 1995 he returned to the Max-Planck-Institute at Mainz. He is a specialist in transmission electron microscopy and his current research interests include water-soluble coatings, latex film characterization, polymer morphology, phase transitions, biomineralization and composites.

Dipl. Chem. Sven Heinz studied chemistry at the University of Regensburg where he received his diploma under the supervision of Prof. Dr. R. Andreesen (Dept. of Haematology and Oncology, University Hospital, Regensburg). In 1996, he joined the group of Prof. Kniep at Darmstadt University of Technology to work in the field of gelatin matrix-assisted biomineralization. In 1997, he returned to the group of Prof. Andreesen where he is currently working on his Ph.D. thesis characterising new dendritic cell-specific gene products.

Dipl.-Ing. Oliver Hochrein studied chemistry at Darmstadt University of Technology, where he received his diploma degree in 1996. He is currently working on his Ph.D. thesis about the synthesis and characterization of nitridometalates. In September 1998 he followed Prof. Kniep to the Max-Planck-Institute for Chemical Physics of Solids at Dresden where he continues his work. Furthermore he is interested in the visualization and simulation of growth processes in biomimetic systems.

Dr. Franco Laeri studied at the University of Bern. He received his Ph.D. degree in 1984 from the Institute of Applied Physics at Darmstadt University of Technology. He then went to IBM in San Jose, USA, and returned to Darmstadt in 1984. His current research interest is centered around the optical and electronic properties of ordered porous materials and nanocomposites.

Dipl.-Ing. Oliver Podebrad studied electrical engineering at Darmstadt University of Technology and received his diploma degree in 1994. Since 1995, he has worked as a research assistant in the department of Theory of Electromagnetic Fields at Darmstadt University of Technology. His main research interest is the numerical calculation of electromagnetic fields with a subgrid-formulation of the Finite Integration Method.

Dipl. Phys. Uwe Vietze studied physics at the Institute of Applied Physics at Darmstadt University of Technology and is a Ph.D. candidate. He obtained his diploma degree in 1994 and his current work involves the optical and electrical properties of ordered porous materials and nanocomposites.



Prof. Dr.-Ing. Thomas Weiland studied electrical engineering and mathematics at Darmstadt University of Technology and received his Ph.D. degree in 1977. As a fellow at the European Institute for Nuclear Research (CERN, Switzerland) he continued his work on electromagnetic computing. In 1983, at the DESY in Hamburg, he founded an international collaboration for 3-D electromagnetic simulations. Since 1989, he is a full professor at Darmstadt University of Technology, as head of the department of Theory of Electromagnetic Fields. In 1993, he was elected a full member of the Academy of Science and Literature at Mainz. He received the "Leibniz-Prize" from the German Research Association in 1987 and the "Max Planck Research Prize for International Collaboration" in 1995.

Prof. Dr. Rüdiger Kniep studied chemistry and mineralogy at the Technical University of Braunschweig and received his Ph.D. degree under the supervision of Prof. Dr. A. Rabenau (Max Planck Institute for Solid State Research, Stuttgart) at the Technical University of Braunschweig in 1973. After his habilitation at the University of Düsseldorf in 1978 he was made a professor of inorganic chemistry in 1979. In 1987 he moved as a full professor of inorganic chemistry to the Darmstadt University of Technology (Eduard Zintl Institute). Since 1998 he is a scientific member of the Max Planck Society and director at the Max-Planck-Institute for Chemical Physics of Solids, Dresden.

MICROREVIEWS: This feature introduces the readers to the authors' research through a concise overview of the selected topic. Reference to important work from others in the field is included.

1. Introduction

The basic principles of biomimetic growth of inorganic solids^{[1][2]} include distinct cooperative phenomena between organic and inorganic components. The complex systems assume control of the processes of self-organization, self-similarity, hierarchical arrangements, shape-formation (form-selectivity) and transcription of informations from the microscopic level to the macroscopic range. In cases where the time scale of the biomimetic morphogenesis of an inorganic material is similar to that in biological systems, the development of specific shapes and morphologies can be systematically investigated from the nucleation to the final stage.

In a recent paper^[3] the biomimetic growth and self-assembly of fluorapatite spheroids by double diffusion in denatured collagen matrices (gelatin) at 25°C was described phenomenologically. The morphogenesis begins with elongated hexagonal-prismatic seeds. Progressive stages of self-assembled (noncrystallographic) upgrowths of needle-shaped prisms at both ends of the seed lead to dumbbell-shaped aggregates, which complete their shapes by successive branchings to end up with spheres that are notched to a greater or lesser extent. A selected sequence of scanning electron microscopy (SEM) pictures representing the morphogenesis from a needlelike seed to a spherocrystal is shown in Figure 1.^{[3][4]} The surface of a just closed sphere also consists of (small) needlelike units following the general principles of self-similarity.

An investigation of numerous SEM pictures at various stages of the morphogenesis has already led to a *fractal model* for the formation of the (anisotropic) fluorapatite spheres.^{[3][4]} Furthermore, according to the previously postulated hypothesis, the fractal branching of successive generations and the overall symmetry of the self-assembled aggregates may be considered as consequences of *intrinsic electric fields*, which take over control of the growth of the aggregates.^{[3][4]} This interpretation of the specific morphogenesis of the fluorapatite aggregates is broadly based on natural phenomena concerning the biological significance of piezoelectricity,^[5] as well as on observations concerning the pyroelectric effect in bone.^[6] In addition, the influence of electric polarization on acceleration and deceleration of bonelike crystal growth on hydroxyapatite ceramics was

also shown in a recent paper^[7] which, in fact, supports the idea that “uniform electric fields, rather than the localized charges usually cited, may determine the sites of crystal nucleation and overgrowth.”^[8]

This paper now makes a careful attempt at a first approach to the interpretation of the following phenomenological observations:

- **First growth stage:** Fractal growth (branching criteria and architecture, see Section 2).
- **Second growth stage:** Core/shell assemblies (formation of concentric shells around the closed spheres of the first stage, see Section 3).
- **Composite character** of the material (see Section 5).
- Formation of **hollow spheres** by “decalcification” of the composite aggregates (see Section 5).
- **Reorganization of denatured collagen** (gelatin) during morphogenesis (see Section 5).

The specific peculiarities of the chemical system under investigation are caused by numerous preceding stages of selection during evolution. This criterion should be kept in mind when studying and assessing the observations and models given in the present paper. It should also be noted at this point that the formation of morphologies similar to that of dumbbell-shaped aggregates or peanut-type particles, which are found in various chemical systems under various chemical growth conditions,^[9] are not necessarily generated by the same mechanism of morphogenesis.

2. Fractal Growth and Architecture

The growth of anisotropic fluorapatite spheres^{[3][4]} by double diffusion in denatured collagen matrices (gelatin) begins with elongated hexagonal-prismatic seeds up to 30 µm in length (critical ratio length/diameter ≈ 5:1). Progressive stages of self-assembled (noncrystallographic) upgrowths of needle-shaped prisms at both ends of the seed (fractal branching) lead to dumbbell-shaped aggregates (Figure 1) which complete their shapes by successive and self-similar upgrowths to give notched spheres after about the 10th fractal generation. The morphogenesis from a needle-shaped seed of about 10 µm in length to a spherocrystal of about 60 µm in diameter takes approximately one week. The fractal growth and architecture is controlled by two noncrystallographic parameters, which were derived from SEM images at different growth stages: i) the maximum aperture angle between the long axis of the seed and the needle-axes of the units of the following generation is $45 \pm (5)^\circ$; ii) subsequent generations scale down in their lengths by a factor of ≈ 0.7. Based on these two limiting conditions the fractal model^[10] of a just closed sphere is shown in Figure 2 (2D-simulation with the umbrella-tree model; crossing of individual crystals suppressed). The simulated surface of the spherocrystal consists of very small needlelike units, an observation which is consistent with the SEM images (mean diameter < 0.1 µm for the surface prisms of a just closed sphere). Inside the spherocrystal a torus-shaped cavity is

^[a] Eduard-Zintl-Institut der Technischen Universität, Hochschulstraße 10, D-64289 Darmstadt, Germany

^[b] Henkel KGaA, TTR-Anorganische Chemie, Henkelstraße 67, D-40191 Düsseldorf, Germany

^[c] Max-Planck-Institut für Polymerforschung, Ackermannweg 10, D-55128 Mainz, Germany

^[d] Institut für Angewandte Physik der Technischen Universität, Schloßgartenstraße 7, D-64289 Darmstadt, Germany

^[e] Fachgebiet Theorie Elektromagnetischer Felder der Technischen Universität, Schloßgartenstraße 8, D-64289 Darmstadt, Germany

^[*] New address:

Max-Planck-Institut für Chemische Physik fester Stoffe (im VEM Sachsenwerk), Pirnaer Landstraße 176, D-01257 Dresden, Germany

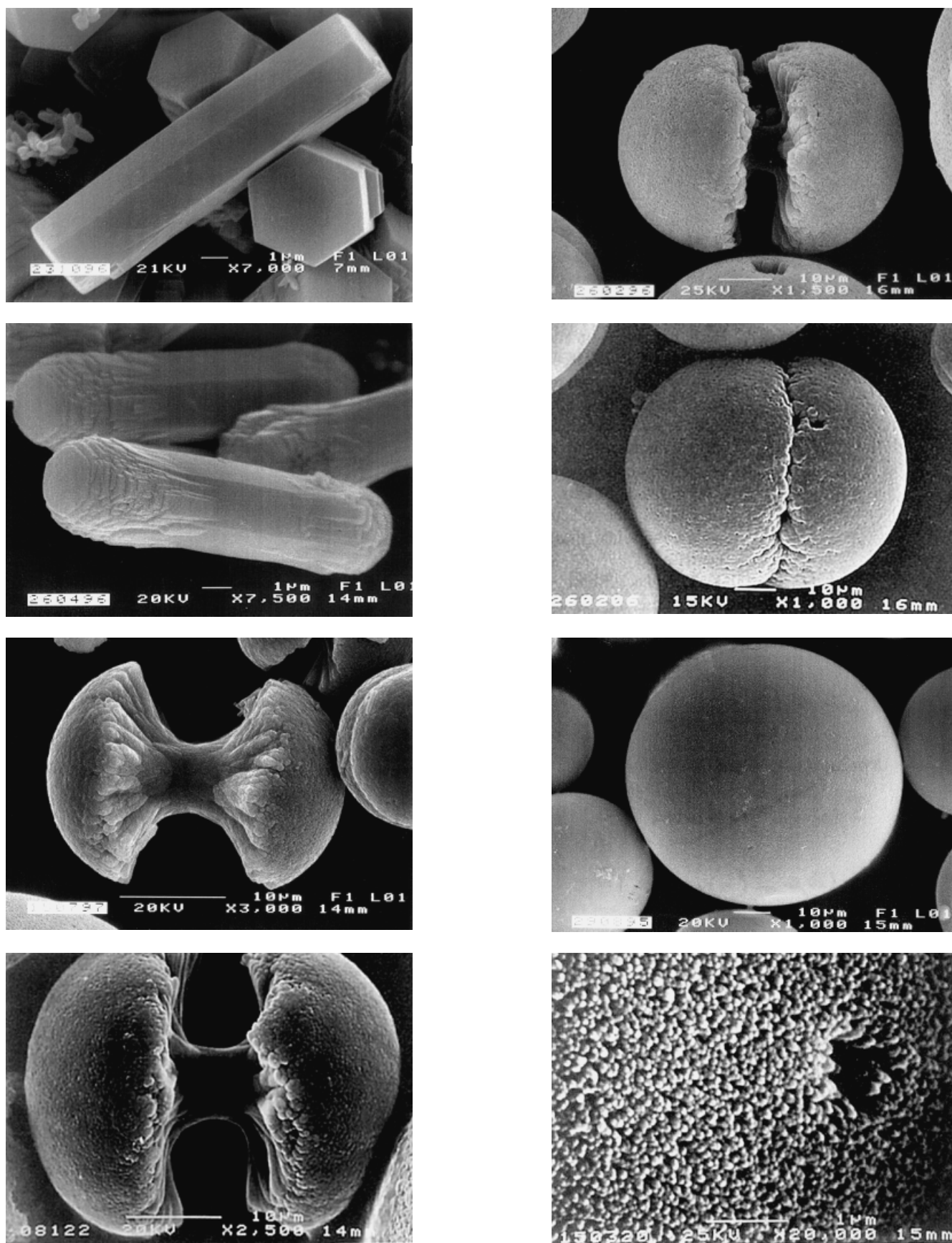


Figure 1. Selected sequence of SEM images of progressive stages of self-assembled (hierarchical) growth of fluorapatite aggregates (morphogenesis): from an elongated hexagonal-prismatic seed (top left) through dumbbell shapes to spheres; the surface of a just closed sphere also consists of needlelike units (bottom right) following the general principles of self-similarity

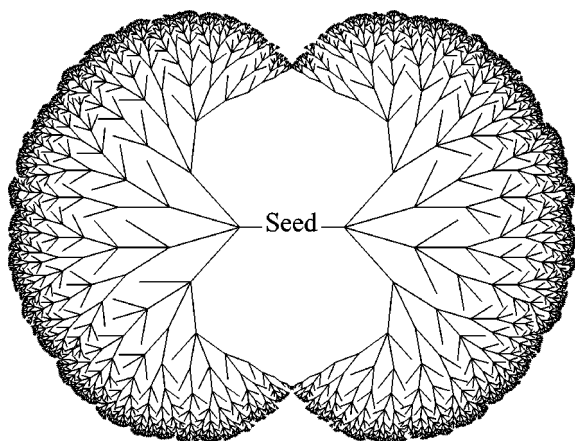


Figure 2. 2D-simulation of a just closed fluorapatite spheroaggregate; fractal model (seed plus 10 generations) assuming a fourfold splitting in each generation (in fact, orders of noncrystallographic branching can be higher); maximum opening angle 48° , scale down factor 0.7; crossing of individuals is suppressed by particular rules following real growth conditions: i. all individuals have the same growing speed; ii. members of higher generations are suppressed, if they cross members of a lower generation; iii. if members of the same generation reach the crossing point at the same time, it is a random decision which one is deleted; if crossing is “nonsymmetric”, the individual reaching the crossing point first is favoured; iv. to simulate diffusion-inhibition inside the growing dumbbell area all individuals with an angle greater than 160° relative to the seed are deleted

formed around the elongated seed. A similar architecture is generated by the geometrical model of a splitting needle at constant growth rate and constant splitting rate.^[11]

Selected stages of the morphogenesis (SEM images), together with more detailed 3D-simulations,^[12] are shown in Figure 3. SEM images of fragments of a spherocrystal are given in Figure 4 and agree very well with the fractal model (Figure 2, Figure 3, Figure 4b). The fragments were produced by breaking spherocrystals perpendicular (Figure 4a) and parallel (in plane; Figure 4d) to the long seed axis. The seed position within a spherocrystal is clearly seen in the centre of the hemisphere (Figure 4a, simulation: Figure 4b). The hexagonal cross-section of the seed and the channel surrounding the seed are shown in Figure 4c. It is interesting to note that the cleavage area of the elongated hexagonal-prismatic seed is characterized by a radial structure starting from the middle, an observation which is in agreement with the idea of nucleation by cylindrical preorientation of macromolecular units (“liquid crystal seed”).^[13] Figure 4d shows an inner-sphere cross-section parallel to the long seed axis; the two holes represent the torus-shaped cavity around the elongated seed between. The complex but symmetric structure of growth (mirror plane perpendicular to the long seed axis and through the holes) corresponds to the fractal model given in Figures 2–4 and will be discussed in more detail later together with the idea of permanent

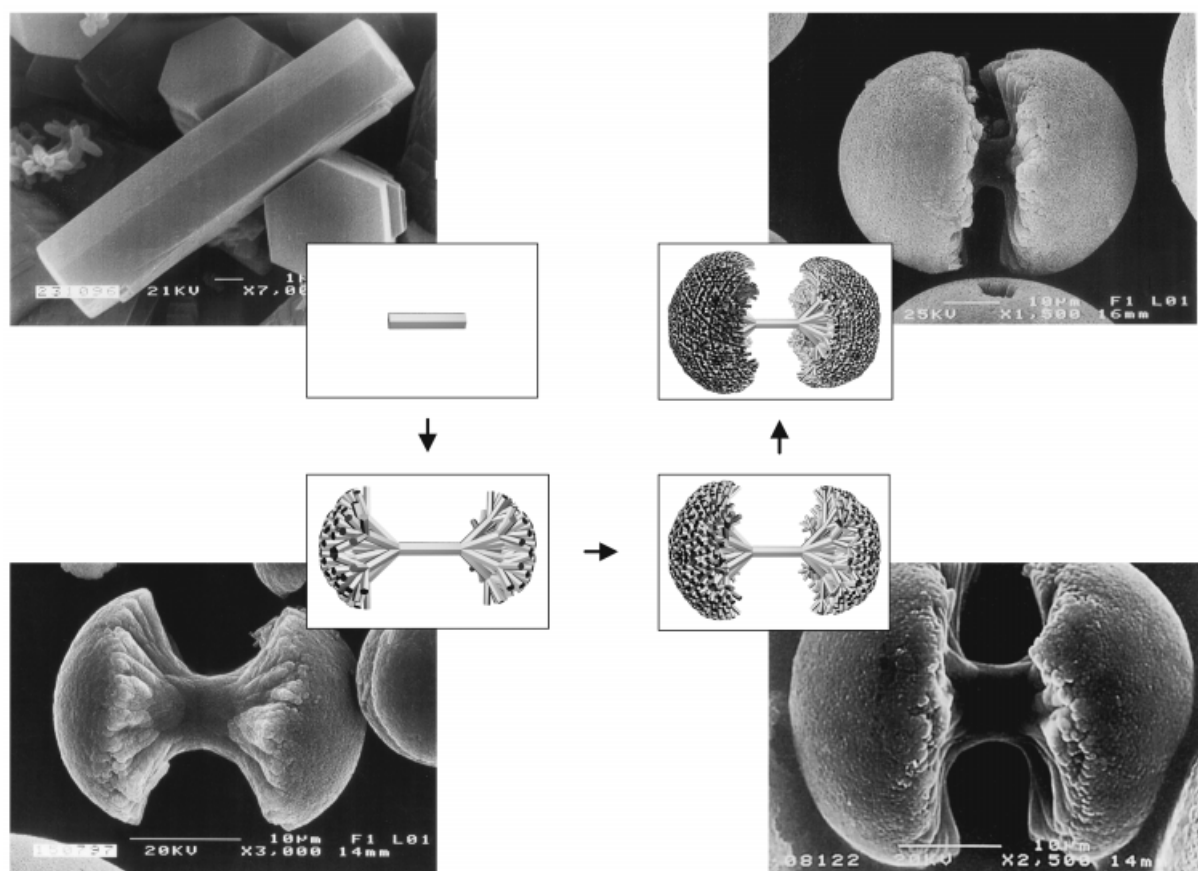


Figure 3. Selected stages of the fractal morphogenesis (SEM images) together with 3D-simulations (from top left anticlockwise: seed, seed + 2, + 3 and + 4 generations)

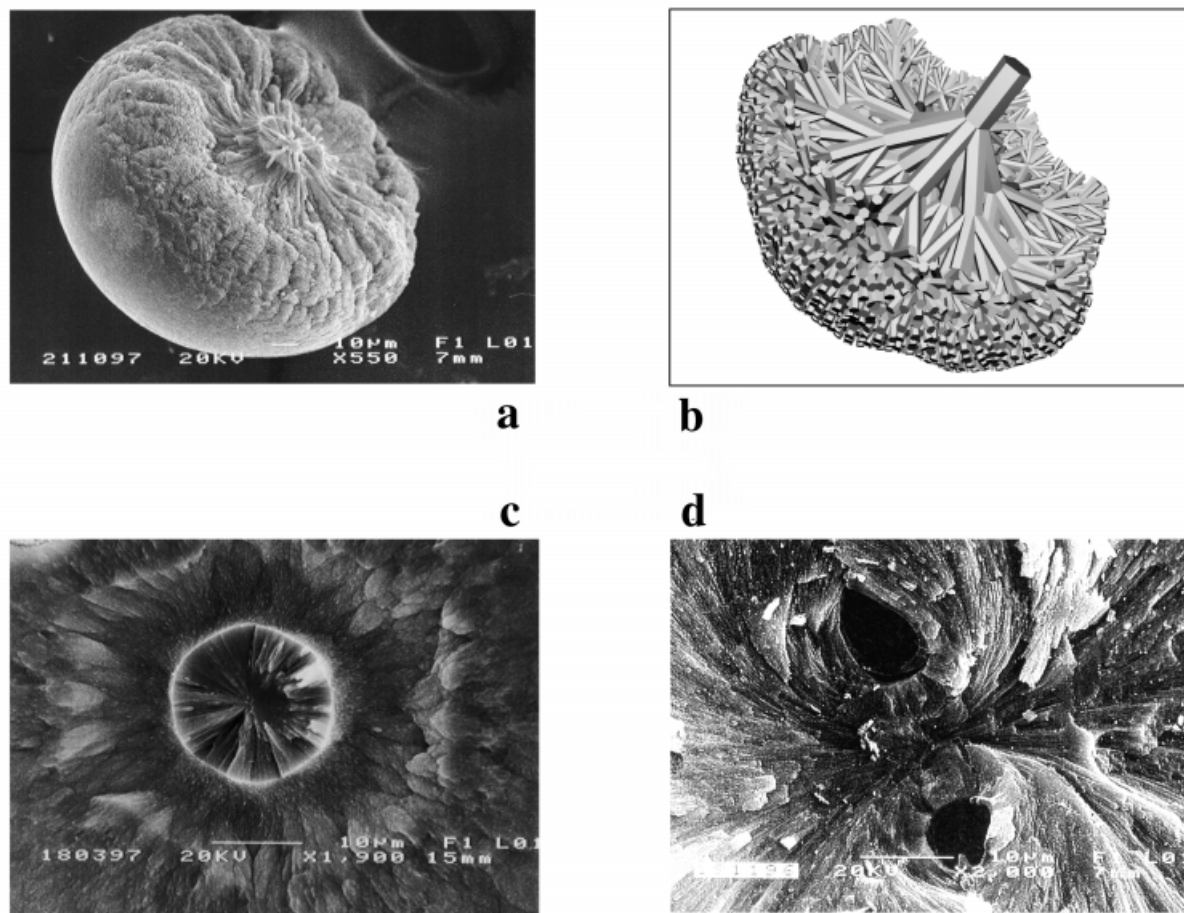


Figure 4. SEM images of specific fragments of a spheroaggregate (fractal model in Figures 2 and 3). **a**: Hemisphere broken perpendicular to the long seed axis; **b**: 3D-simulation^[12] of situation **a** (seed + 4 generations); **c**: Hexagonal shaped cross-section of the seed and surrounding channel; **d**: Inner-sphere cross-section parallel (in plane) to the long seed axis

dipoles and their influence on morphogenesis. Here, only a brief comment is given concerning the inner architecture of the spherocrystal (Figure 4d) and the distribution of electric field lines around a given permanent dipole. This situation is demonstrated in Figure 5, in which the growth-orientation within a spherocrystal (section parallel/in plane to the seed) shows a remarkable correspondence to the orientation of electric field lines around a permanent dipole.

3. Core/Shell Assemblies

After the spherocrystals have closed, this special kind of fractal morphogenesis no longer applies and a second, more conventional, growth mechanism by the formation of concentric shells^[14] of fluorapatite around the core follows (Figure 6). The shells are built of needle-shaped rods oriented perpendicular to the core-surface and nearly parallel to each other (radial growth). Obviously, the small needle-shaped prisms of the last generation of the fractal core act as nucleation centers for the growing shell. The core/shell interface represents a sphere of decreased stability against thermal and/or mechanical treatment. In fact, the core is easily removed from the shell (Figure 6). Simultaneously,

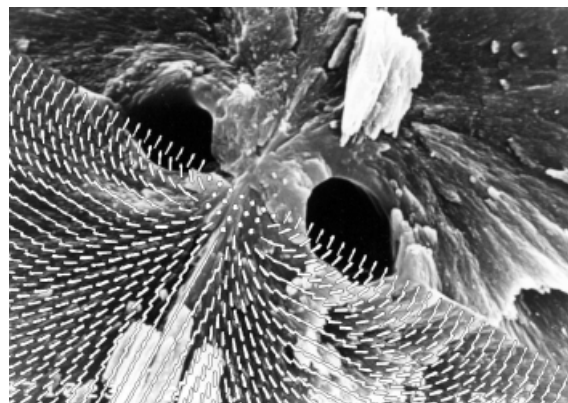


Figure 5. SEM image of a bisected spherocrystal broken parallel (in plane) to the long seed axis (Figure 4d) combined with the calculated shape of electric field lines around a permanent dipole (field lines reduced to only one half of the complete area)

the core and shell assemblies bear a strong resemblance to the complex organisation of teeth (dentin- and enamel).^[15] Bundles of needles are combined in bigger assemblies in the same way as the small prisms in enamel are aggregated to enamel rods (Figure 7).

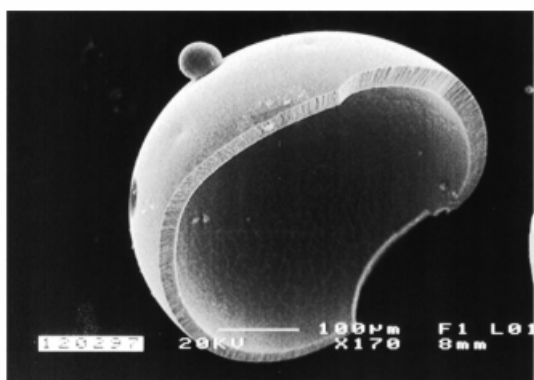
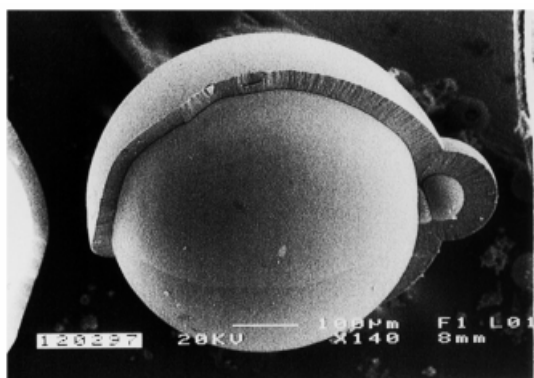


Figure 6. SEM images of a core/shell assembly. a: Shell partly removed, free core; b: Core removed from the shell

4. Intrinsic Electric Fields

Coming back to the core spherocrystal and its architecture, the essential task is to find an interpretation for the

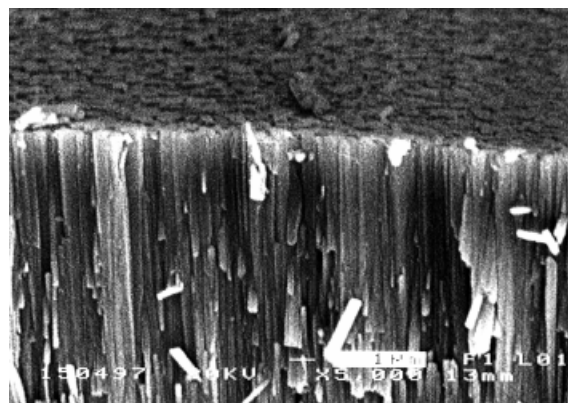


Figure 7. SEM image: Section of a shell area and the surface of a core/shell assembly

noncrystallographic (fractal) splitting of crystal generations and for the overall symmetry ($C_{\infty h}$) of the self-assembled core aggregates. The basic premise in this hypothesis is the presence of intrinsic electric fields which take over control of the growth of the aggregates. This means that the individual “crystals” (actually composite units, see below) – the seeds as well as individuals of the following generations – contain a permanent dipole, an assumption which is consistent with observations on the biological significance of electric fields (pyro-, piezoelectricity) during apatite formation under in vivo or biomimetic conditions.^[5–8] The polarity of collagen and the structural peculiarity of the apatite family, varying between centrosymmetric and acentric distribution of the X-species $\{Ca_5(X)[PO_4]_3, X = F, Cl, OH\}$ ^[16] support these ideas. We should also bear in mind the extremely mild biomimetic growth conditions, which should favour a high degree of order of the atomic arrangements – partial substitution of F^- by OH^- causes an

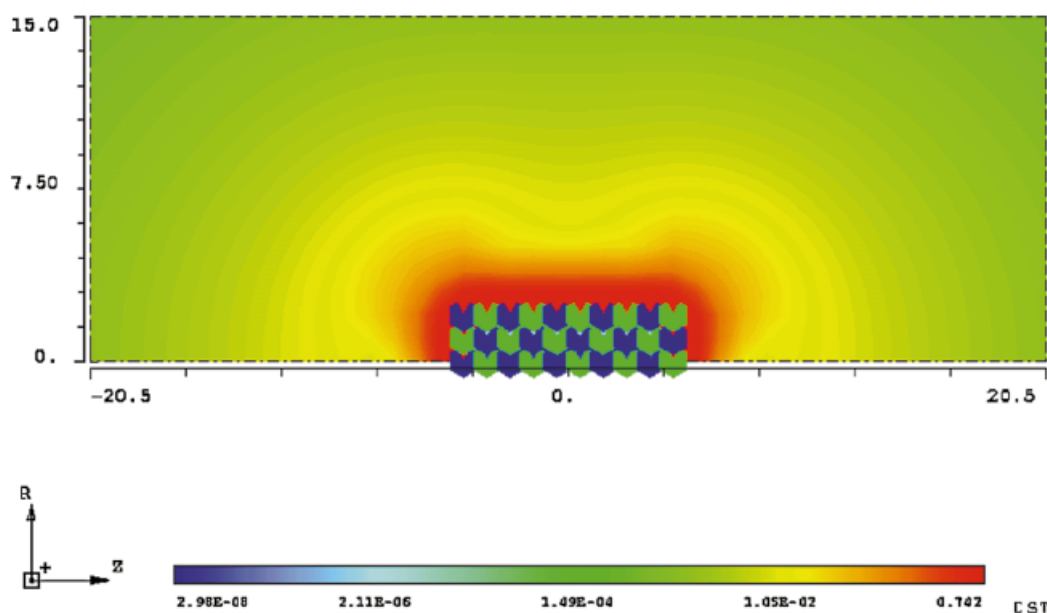


Figure 8. Two-dimensional, logarithmic representation of the distribution of the electric field strengths around an elongated permanent dipole (seed). Elementary dipoles (blue/green graphs = charges $+/-$; staggered arrangement along the horizontal direction) represent the seed within the coloured area; calculation using the MAFIA program.^[19]

asymmetric displacement of the X-species from their "normal" positions (mirror planes)^[17] causing a possible reduction of symmetry from the centrosymmetric point group 6/m to the pyroelectric point group 6. Finally, the polar organic component and the inorganic material may act together in the sense of an ordered composite structure, which then gives rise to the formation of a strong (intrinsic) permanent dipole. In this context it is important to note that in vivo nucleation and growth of apatite nanocrystals within a collagen fibril structure leads to an ordered composite system with the *c* axes of the apatite particles oriented parallel to the long axes of the collagen fibrils.^[18]

The distribution of the electric field strength around an elongated seed with a permanent dipole (simulation by a set of elementary dipoles; staggered arrangement) was calculated using the MAFIA program^[19] and is shown in Figure 8 as a coloured chart of the intensity of the dipole field. Because the field strength is higher at the poles than between them, a bonelike shape results with the maximum field intensities at the edges. The bonelike extension of areas of stronger field strengths starting from the edges of the seed (red/orange in Figure 8) corresponds directly to the self-assembled upgrowths at both ends of the seeds (fractal branching) during progressive growth of the fluorapatite aggregates. Even the maximum aperture angle between the long axis of the seed and the needle axes of prisms of the following generation of about $\pm 45(5)^\circ$ is in agreement with the general direction of the extension of higher field strengths around the elongated permanent dipole.

A two-dimensional simulation of the morphogenesis of the overall orientation of electric field lines around a growing spherocrystal is shown in Figure 9 [Permanent dipoles and fractal branching: seed (a); seed + 2 generations (b); seed + 3 generations (c)]. These diagrams give an impression of the possible interactions between the intrinsic electric fields, the charged or polar components in solution, and the growing aggregate within the gelatin matrix. The following points seem to be of significance and, in principle, are consistent with the observed morphogenesis of the fractal solid: i) the transport of ions from the solution to the growing seed (aggregate) and the reorientation of polar organic molecules are influenced by the strength and direction of the electric fields; ii) electric field lines with an orientation between "parallel and perpendicular" to the seed (to the individuals on top of the growing surface of the spherocrystal) do not contribute to a preferred growth rate; iii) the lack of preferred orientation of the electric field lines inside the growing spherocrystal causes reduced growth rates within this area and formation of the torus-shaped cavity.

Experimental indications for the significance of intrinsic electric fields, which assume control of the growth of the fractal spherocrystals, were obtained by using a modified growth-chamber (Figure 10) including an external electric field of 5000 V/1.4 cm (D.C. conditions). The idea was to influence fractal branching of the growing aggregates, and, in fact, splitting of the seeds (area of high field strengths at the edges of an elongated permanent dipole, Figure 8) is

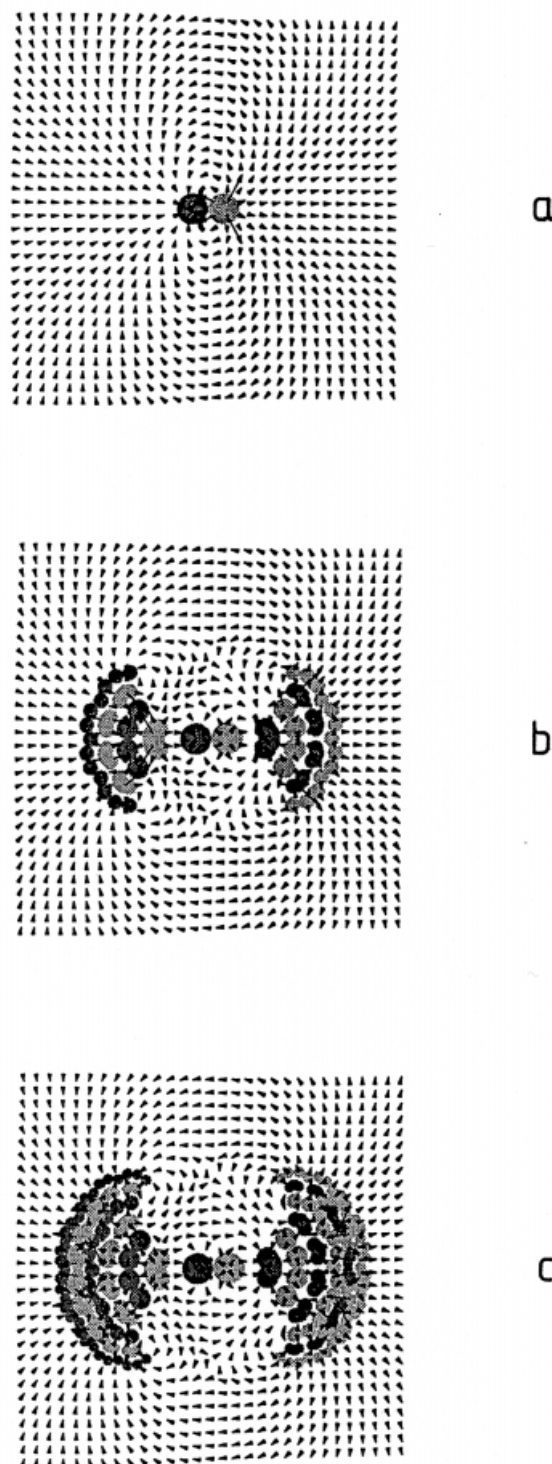


Figure 9. Two-dimensional calculation of the morphogenesis of the overall orientation of electric field lines around a growing spherocrystal; every permanent dipole is represented by a combination of two circles (black/grey circles = charges +/–). a: seed; b: seed + 2 generations; c: seed + 3 generations; arrows show the directions of the electric field lines; no distinction is made for field strengths (see Figure 8)

predominantly affected by the external field (Figure 11). Instead of similarly shaped polyhedra with definite prism and basal planes, the upgrowing generation under an external

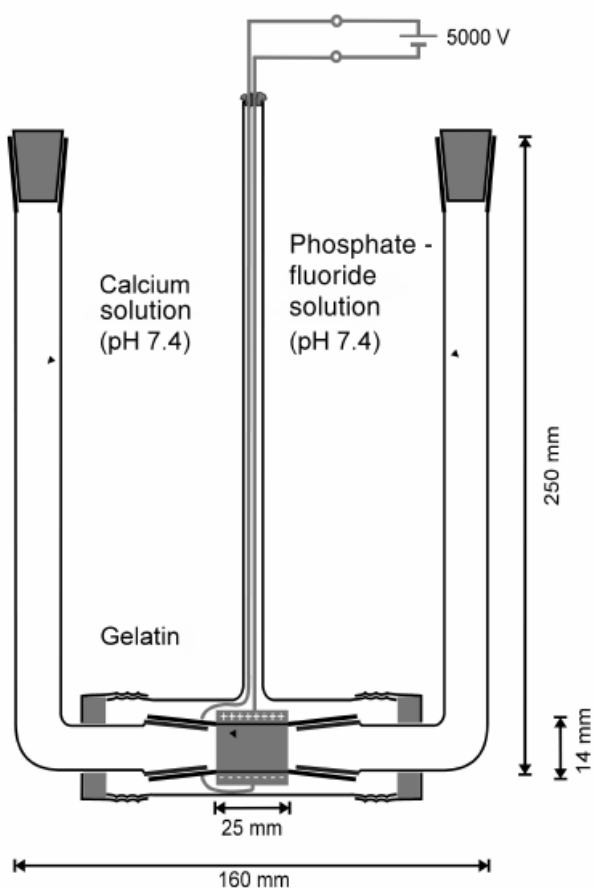


Figure 10. Modified growth chamber (double diffusion technique) including the facility for application of an external electric field (5000 V/1.4 cm; D. C. conditions); the electrodes are placed on opposite sites of the horizontal glass tube which contains the gelatin plug; to prevent contact with moisture the electric circuit is protected by an outer glass envelope; the equipment is suitable for use in thermostats operating with water

field is characterized by sharpened and bent faces. Moreover, the growing rate of fluorapatite aggregates is significantly diminished by using an external field.

If the spherocrystals (fluorapatite-gelatin composites, see below) represent solid aggregates containing a permanent dipole, a pyroelectric effect similar to that observed in bone and other collagen-containing materials^[6] should be expected. We therefore developed an experimental setup for measuring the pyroelectric effect of small aggregates (down to 100 μm in size).^[20] The sensitivity of the equipment is already suitable for determining the pyroelectric coefficient of small particles of tourmaline (4.3×10^{-10} coul. $\text{cm}^{-2}\text{C}^{-1}$); however, the expected order of about $2-4 \times 10^{-13}$ coul. $\text{cm}^{-2}\text{C}^{-1}$ for bonelike materials^[6] has not yet been attained. On the other hand, we were able to get an experimental indication for the presence of a permanent dipole in the spherocrystals by placing them in a high-voltage field between two condenser plates. As shown in Figure 12 an applied voltage of 5 kV/cm leads to chainlike arrangements of the spherocrystals. The spherocrystals within the chains are mainly oriented in such a way that the

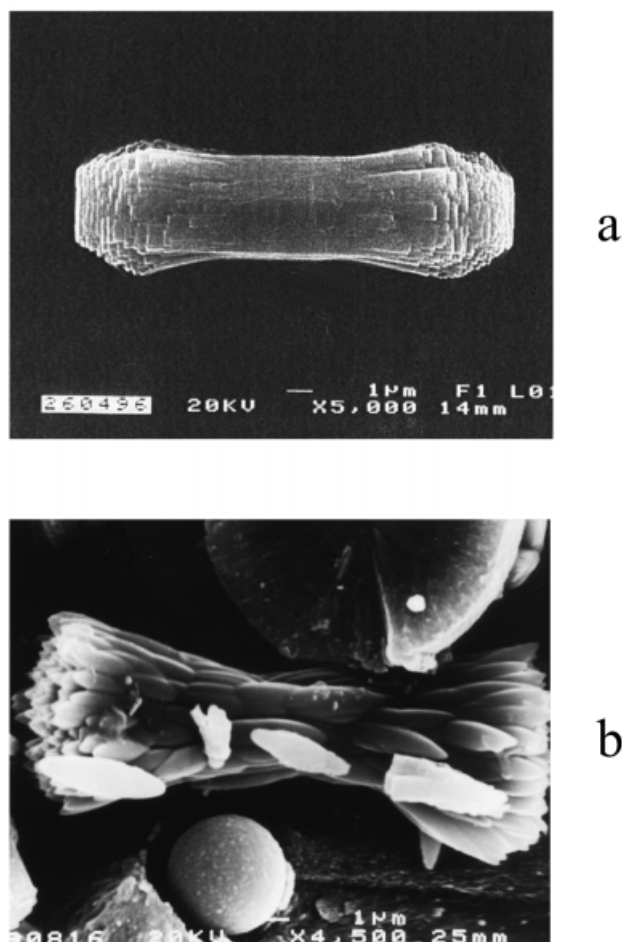


Figure 11. SEM images of fluorapatite seeds together with the first upgrowing generation. a: without external field. b: with applied external field (5000 V/1.4 cm)

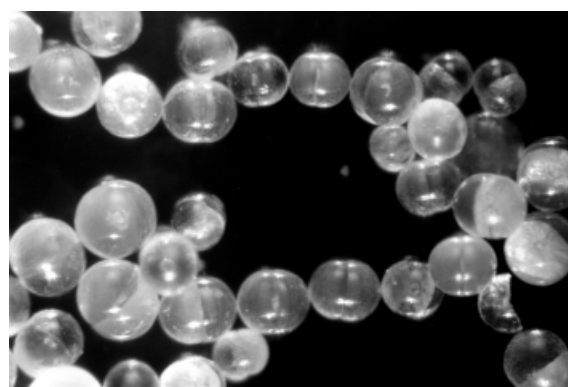


Figure 12. Orientation of fluorapatite spherocrystals exposed to an external high-voltage field of 5 kV/cm (horizontal field); max. sphere-diameter: 400 μm

elongated seeds of the spheres (in a direction perpendicular to the equatorial grooves) are in a parallel arrangement, a picture which is consistent with the expected orientation of rod-shaped permanent dipoles between condenser plates.

5. Composite Character, Hollow Spheres and Reorganization of Denatured Collagen during Morphogenesis

The experimental indications for the presence of permanent dipoles and intrinsic electric fields are one of the specific characteristics of the spherocrystals and their morphogenesis. The second essential point is to gain further insight into the composite-nature of the spherocrystals. As already shown by thermogravimetry,^{[3][4]} the biomimetically-grown spherocrystals consist of about 95 wt.-% fluorapatite and about 5 wt.-% organic material and water. A similar ratio of inorganic and organic material is found for human enamel.^[21] The composite structure of the spherocrystals is also reflected by dissolution processes in EDTA (0.25 N, pH = 7) as solvent for the inorganic component. Two main observations have been made on treatment of fluorapatite spheres with a neutral EDTA solution at 25°C; they concern firstly the dissolution of the fluorapatite spheres and secondly the structural correlation between apatite and gelatin.

the first stage of the dissolution process the seed within the core is only weakly affected; the later generations of the fractal core spherocrystal are obviously dissolved first (a). After the core has been completely dissolved the attack of the solvent extends to the shell structure and the dissolution progresses leading to a decrease of the wall thickness and an increase of the cavity area (b-d). Decreasing thickness of the "inorganic wall" is consistent with increasing elasticity of the spheres in solution; the consistency of the completely "decalcified" and translucent spheres is similar to that of jellyfish. The early stages of the dissolution process of the fluorapatite core/shell assemblies show close similarities to the early effects of caries:^[22] while the surface of a tooth might still be intact, a cavity is formed in the underlying parts. This mechanism occurs in hydroxyapatite-containing teeth as well as in shark teeth (fluorapatite), as was shown by an *in vitro* study of simulated caries attacks.^[23] It was also supposed^[24] that the decomposition products of bacteria and their complexing properties are responsible for caries. In the course of these investigations^[24] caries-like lesions were obtained by using EDTA as a model reagent.

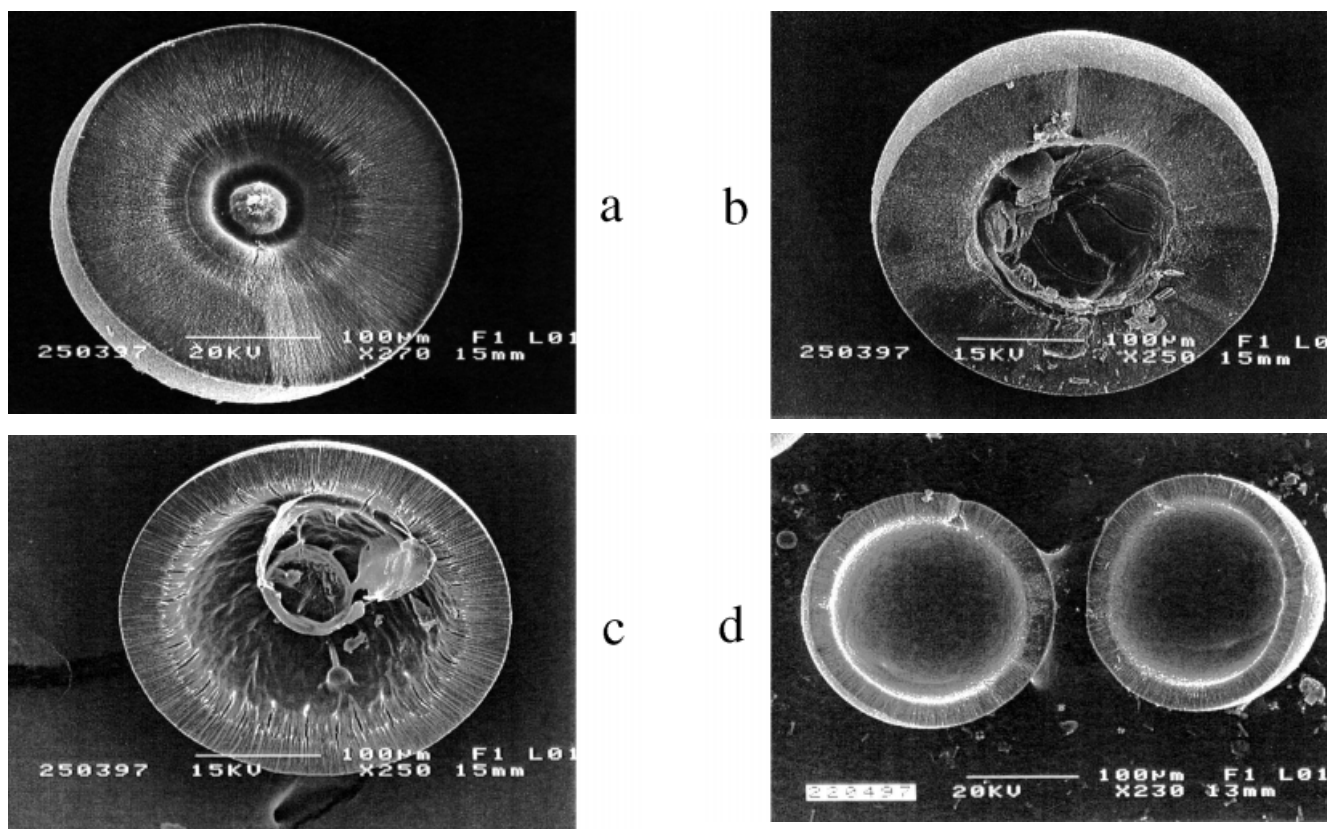


Figure 13. Dissolution of fluorapatite core/shell assemblies in EDTA as solvent; SEM images of hollow hemispheres broken from spheres after treatment with EDTA for 24 h (a), 48 h (b), 72 h (c) and 96 h (d); picture (d) represents the two hollow hemispheres of the same individual; due to shrinking effects during the preparation for SEM investigations (drying) the residual gelatin inside the core loses its original (biomimetic) structure

The first observation is that the dissolution of core/shell assemblies starts within the core and spreads out to the shell, thereby running through continuous stages of apatite hollow-spheres filled with residual gelatin. This situation is shown in Figure 13, which represents hollow hemispheres broken from spheres at different stages of dissolution. In

The second major observation concerning the composite nature of the spherocrystals gives a first answer to the question whether there is a structural correlation between apatite and gelatin. Figure 14 shows images (optical microscope with crossed polarizers) of closed composite core aggregates (a) and of the jellyfish-like spheres (b) obtained

after complete dissolution of the apatite component. The gelatin spheroids show a significant anisotropic optical behaviour (Brewster cross) identical to undissolved spherocrystals but without interference colours because of the lack of the inorganic material. Hence there is a strong structural correlation between the orientation of apatite crystallites and the gelatin within the composite spheres, indicating substantial reorganization of the macromolecular matrix within the area of a growing aggregate. Birefringence analyses (λ plate) of partially dissolved and broken specimens show that the directions of the optically denser axes in the apatite crystallites (c axes) and the gelatin (chain direction) coincide, as would be expected if the gelatin was preferentially oriented during the process of apatite growth.

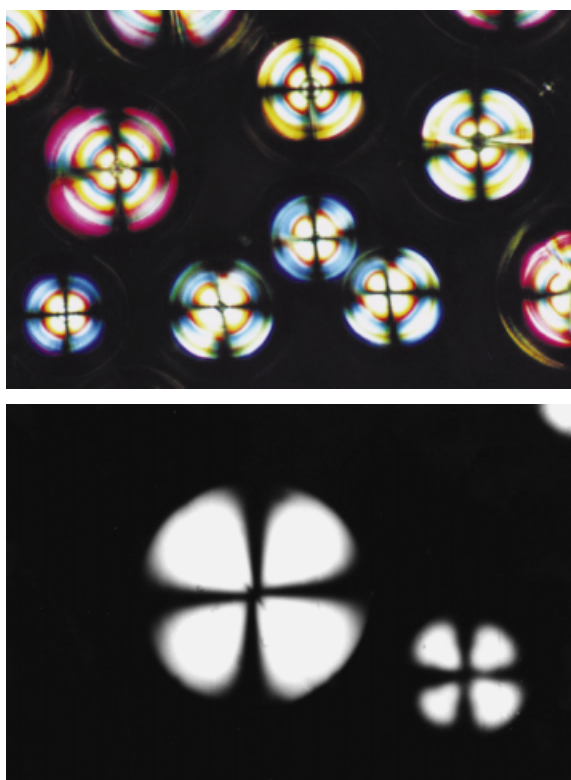


Figure 14. Images from a polarization microscope (crossed polarizers) of just closed composite spheres (apatite/gelatin; a) and of completely "decalcified" spheres (gelatin; b); the gelatin spheroids (b) show significant anisotropic behaviour (Brewster-cross) identical with that of the undissolved spherocrystals (a) but without interference colours because of the lack of inorganic material (apatite); sphere diameters between 100 μm and 150 μm

For transmission electron microscopy (TEM) investigations the composite spherocrystals were first separated from the gelatin matrix by pressing them through a screen and treating them with water. Prior to the dissolution process with EDTA the isolated spheres were immediately fixed with glutardialdehyde and subsequently contrasted with osmium tetroxide. The water was then extracted by gradual exchange with acetone and the spheres embedded in epoxy resin. Ultrathin sections were prepared at low temperature and subsequently stained with uranyl acetate. In Figure 15 parallel alignments of residual apatite crystallites are visible within a matrix of embedding material and stained gelatin

forming a dark network. Within this network stripes are discernible giving the impression of a gelatin structure oriented parallel to the longitudinal axes (c axes) of the apatite crystallites. It is thought that the preparation does not change the original gelatin structure of the composite significantly and hence it is assumed that the structure visible in Figure 15 represents the distribution of gelatin within the composite together with apatite. The combination of the TEM observations with the results of optical microscopy leads us to conclude that the stripes (Figure 15) are bundles of gelatin which are stressed and ordered in a parallel orientation together with areas of crystalline apatite. This means that the growth of the aggregates is associated with significant interactions between apatite and gelatin, which cause a reorientation of gelatin from an irregular (amorphous) to an ordered (anisotropic) state.

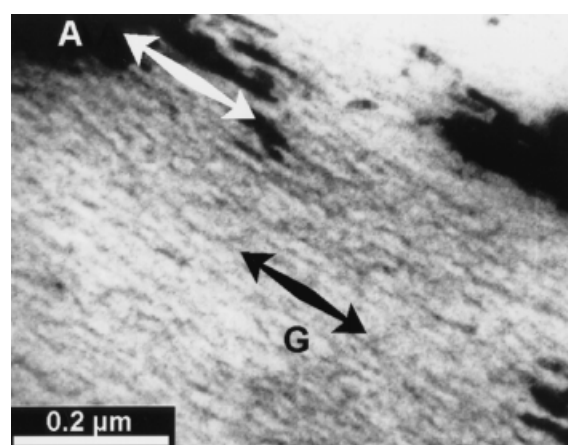


Figure 15. TEM image of an ultrathin section of an apatite/gelatin composite spherocrystal after treatment with EDTA (partial dissolution of the inorganic component, for preparation see text); "A" represents an area of residual apatite crystallites with their longitudinal axes (c axes) parallel to the bright arrow; the stained gelatin region "G" shows an overall orientation (black arrow) parallel to the apatite longitudinal axes

6. Concluding Remarks

In summary, the apatite-gelatin system seems to be well suited for a wide range of interdisciplinary studies to gain further insight into the principles of the morphogenesis of a complex biomimetic material. This story is just beginning and there are still a lot of questions, as can also be seen in the title of the present paper!

Before coming to the end of this contribution only one peculiarity, which may include the key to the deeper understanding of the mechanism of the morphogenesis, should be emphasized in more detail. Though the seed units of the fractal aggregates are formed with a perfect hexagonal-prismatic habit they do not correspond to a single crystal, a fact which is demonstrated by the specific appearance of the fracture area perpendicular to the seed axis (Figure 16). The radial structure of the fracture area indicates that the nucleation of a hexagonal-prismatic unit starts from a central seed which may be formed by fibril-analogue arrange-

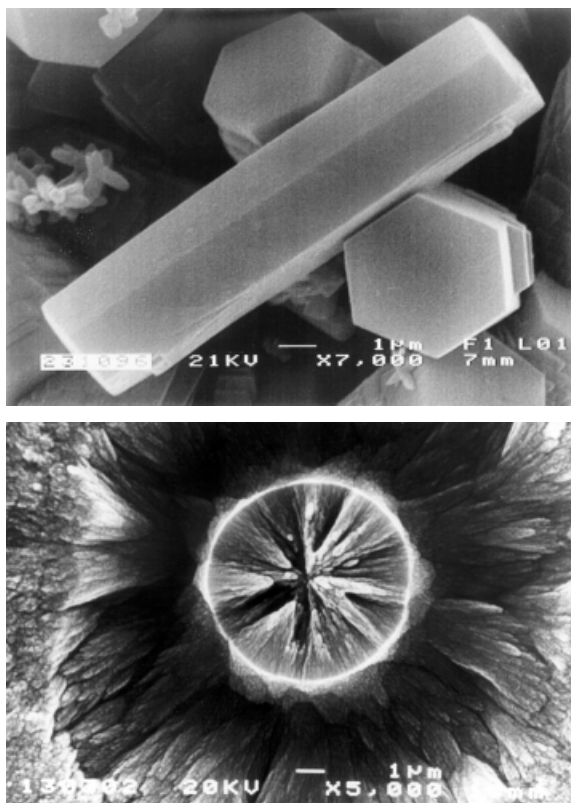


Figure 16. SEM images: Hexagonal prismatic seed (top) and fracture area of a seed (bottom) nearly perpendicular to the seed axis

ments of gelatin molecules able to provide active centres for the nucleation of apatite. The actual size of the apatite crystallites formed is not defined at present and may extend from the nanoscopic to the mesoscopic scale. If this low-scale composite model is valid, the macroscopic hexagonal-prismatic seed is not a single crystal but a hierarchically ordered inorganic/organic composite superstructure. This important question will be the central subject of our future investigations.

Acknowledgments

This work was supported by the Fonds der Chemischen Industrie.

- [1] S. Mann, *J. Chem. Soc., Dalton Trans.* **1997**, 3953–3961.
 [2] N. Coombs, D. Khushalani, S. Oliver, G. A. Ozin, G. C. Shen, I. Sokolov, H. Yang, *J. Chem. Soc., Dalton Trans.* **1997**, 3941–3952.
 [3] R. Kniep, S. Busch, *Angew. Chem.* **1996**, *108*, 2787–2791; *Angew. Chem. Int. Ed. Engl.* **1996**, *35*, 2624–2626.
 [4] S. Busch, Ph. D. Thesis, TU Darmstadt 1998.
 [5] C. A. L. Bassett, *Calc. Tiss. Res.* **1968**, *1*, 273–287.
 [6] S. B. Lang, *Nature* **1966**, *12*, 704–705.
 [7] K. Yamashita, N. Oikawa, T. Umegaki, *Chem. Mater.* **1996**, *8*, 2697–2700.
 [8] P. Calvert, S. Mann, *Nature* **1997**, *386*, 127–129.
 [9] *Apatite*: K. Schwarz, M. Epple, *Chem. Eur. J.* **1998**, *4*, 1898–1903; *ZSM-48*: V. J. Hufnagel, P. Behrens, *10th German Zeolite Conference* (Bremen), **1998**, Abstract A6; *a-Fe₂O₃*: N. Sasaki, Y. Murakami, D. Shindo, T. Sugimoto; *J. Coll. Interface Sci.* **1999**, *213*, 121–125; *BaSO₄*: L. Qi, H. Cölfen, M. Antonietti, *Angew. Chem.*, in press.
 [10] B. B. Mandelbrot: *Die fraktale Geometrie der Natur*, Birkhäuser Verlag, Basel, **1991**.
 [11] M. N. Maleev, *Tschermaks Min. Petr. Mitt.* **1972**, *18*, 1–16.
 [12] POVRAY 3.1e©, **1991–1999**, The Persistence of Vision Team, <http://www.povray.org>.
 [13] G. A. Ozin, H. Yang, I. Sokolov, N. Coombs, *Adv. Mater.* **1997**, *9*, 662–667.
 [14] W. J. Schmidt, *Naturwiss.* **1947**, *9*, 273–277.
 [15] H. E. Schroeder: *Orale Strukturbiologie*, Thieme Verlag, Stuttgart/New York, **1982**.
 [16] M. Bauer, W. E. Klee, *Z. Kristallogr.* **1993**, *206*, 15.
 [17] M. Braun, C. Jana, *Chem Phys. Lett.* **1995**, *245*, 19.
 [18] *Biomimetic Materials Chemistry* (Ed.: S. Mann), VCH Publishers Incorp., New York, **1996**.
 [19] The MAFIA collaboration, User's Guide MAFIA Version 4.X, CST Gesellschaft für Computer-Simulationstechnik mbH, Lautenschlagerstr. 38, D-64289 Darmstadt.
 [20] F. Laeri: Measurement of the pyroelectric effect of small particles, unpublished.
 [21] M. Okazaki, J. Tokahashi, H. Kimura, *J. Osaka Univ. Dent. Sch.* **1989**, *29*, 47–52.
 [22] N. Schwenzer: *Zahn-, Mund-, Kiefer-Heilkunde*, Bd. 4, Thieme-Verlag, Stuttgart/New York, **1988**.
 [23] J. G. Clement, D. J. Langdon, A. Thistleton, *Caries Res.* **1981**, *15*, 451–452.
 [24] A. Schatz, J. J. Martin, *Bl. Zahnheilkunde* **1965**, *26*, 191–203.
 Received March 28, 1999
 [199160]